On determining conditions for RRKM behavior in conservative dynamical systems[a)]

Nelson De Leon[b)] and Bruce J. Berne

Department of Chemistry, Columbia University, New York, New York 10027
(Received 5 August 1981; accepted 24 February 1982)

It is shown that a simple linear analysis on certain elliptic fixed points can be used to determine when a system will not exhibit a rate constant that is well approximated by RRKM theory. This method is used to locate those regions in parameter space where RRKM theory is expected to be valid.

I. INTRODUCTION

Recently, there has been considerable interest in the reaction dynamics governing isomerization reactions.[1-6] In particular, interest has focused not only on the extraction of rate constants, but also on their relation to the nonlinear dynamical aspects of the problem, e.g., the KAM theorem, invariant tori, etc. We have recently completed a study of a two degree of freedom system capable of undergoing isomerization.[2] Attention was focused on the conditions necessary for a phenomenological rate constant to exist. Several qualitative conclusions were arrived at in that study. Of particular interest, we found that in order for a rate constant to exist, the energy must be close to the energy of the barrier, and, moreover, a significant measure of the invariant tori must be destroyed. In fact, when all of the invariant tori are destroyed, then the rate constant for the reaction agrees well with the RRKM rate constant prediction.[7,8]

In this paper, we study a similar double well system, but with the added feature that, for this system, it is analytically possible to predict, with some accuracy, when one can expect the system to be an RRKM system. This analyticity is, of course, desirable, since it allows us to investigate and qualitatively predict the statistical behavior of the rate constants as a function of the parameters in the Hamiltonian.

II. RATE CONSTANTS

Consider an isomerization reaction of the kind

$$\mathrm{A} \underset{k_{\mathrm{A}\to\mathrm{B}}}{\overset{k_{\mathrm{A}\to\mathrm{B}}}{\rightleftharpoons}} \mathrm{B} \ . \tag{1}$$

It is assumed that along the reaction coordinate one has a double well potential. The left-hand well is labeled "A" and the right-hand well is labeled "B." For isolated molecules, the reactive flux across the barrier $K(t)$ is given by[1,2,4,5]

$$K(t) = \langle \dot{q}(0)\delta[q(0) - q_{\mathrm{TST}}] H_{\mathrm{B}}[q(t)] \rangle \ . \tag{2}$$

In the above equation, q is the reaction coordinate, q_{TST} is the value of q at the transition state, and $H_{\mathrm{B}}[q(t)]$ is the characteristic function which is unity if $q(t) = \mathrm{B}$ and 0 otherwise. The brackets $\langle \cdots \rangle$ denote a canonical or microcanonical ensemble average. In this paper, we will be dealing with the microcanonical ensemble. If after a sufficiently long time $K(t)$ decays as an exponential $K(t) \sim \exp(-t/\tau_{rxn})$ then the decay constant $1/\tau_{rxn}$ is related to the rate constants $k_{\mathrm{A}\to\mathrm{B}}$ and $k_{\mathrm{A}\leftarrow\mathrm{B}}$ by

$$\begin{aligned} k_{\mathrm{A}\to\mathrm{B}} &= x_{\mathrm{B}}/\tau_{rxn} \ , \\ k_{\mathrm{A}\leftarrow\mathrm{B}} &= x_{\mathrm{A}}/\tau_{rxn} \ , \end{aligned} \tag{3}$$

where x_{A} and x_{B} are the equilibrium mole fractions of A and B, respectively.

The RRKM value for the rate constant is easily calculated by evaluating $K(t)$ in the limit $t \to 0+$. The result is

$$k_{\mathrm{A}\to\mathrm{B}} = \lim_{t\to 0+} K(t)/x_{\mathrm{A}} \ . \tag{4}$$

In the next section, we briefly discuss some of the results from Ref. 2 that are pertinent to this paper.

III. BISTABLE-MORSE SYSTEM

In Ref. 2, a detailed study was made of a dynamical system of two degrees of freedom consisting of a quartic bistable oscillator coupled to a Morse oscillator. Trajectories, fluxes, and rate constants were computed and compared. The analysis was based upon the variation of two parameters, a perturbation strength Z and a Morse parameter λ. Figure 1 displays some typical results. In the first column, we plot the Configurational Surface of Section (CSS). The CSS is defined to be the mapping of all trajectories of energy E on to the configurational plane (X, Y). It is generated by plotting the values X, Y whenever $\dot{X} = 0$ and $\dot{Y} > 0$ (see Ref. 2 for details). The outer curve is the equipotential at the energy of interest. All of the CSS in Fig. 1 were taken at a dimensionless energy of 1.02 units (0.02 units above the barrier). A regular trajectory is characterized by a pair of (parallel) curves, whereas an irregular trajectory is characterized by a set of random points in the CSS. The CSS depicts those parts of the configurational plane where a given trajectory is at a turning point along the X mode. It should be pointed out that the CSS is not, in contrast to the usual Poincare surface of section in q, P space,[9] an area preserving mapping. Its utility does not lie in this feature, but rather on the qualitative aspects of the dynamics that it clarifies, e.g., one can readily note where in configuration space an irregular (or regular) trajectory may or may not visit. The hatched regions of the CSS depict those regions where "irregular" trajectories

[a)]Supported by a grant from the National Science Foundation (NSF CHE 79-07820).
[b)]Present address: Department of Chemistry, UCLA, Los Angeles, California 90024.

 0021-9606/82/130283-07$02.10

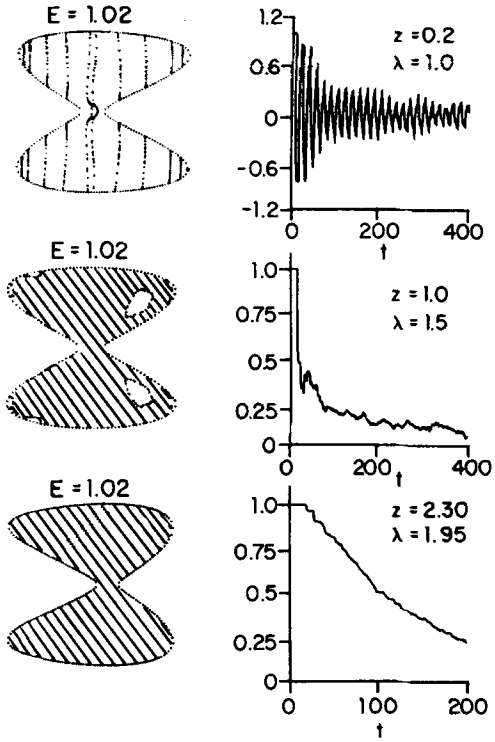

FIG. 1. In this figure, a brief comparison is made between the dynamical structure and the corresponding microcanonical reactive flux $K(t)$ for the system of Ref. 2. All three of these systems are at a total energy of 1.02 units (0.02 units above the barrier). The mapping of the invariant tori in the configurational plane; i.e., the CSS (see the text) are given in the first column. The hatched regions correspond to regions accessible by irregular trajectories. The bottom two systems allow for a high degree of irregularity, whereas the top system allows for very little or none. Note the dramatic difference in the behavior of the corresponding fluxes. The values of Z and λ are taken from Ref. 2.

are found and the curves made up of dots depict periodic or quasiperiodic trajectories. In the bottom two sections of Fig. 1, trajectories of the latter type lie on invariant tori located inside one well. A torus of this type has been labeled a "trapping torus." For instance, if an irregular trajectory is superimposed on the CSS, one will find that the trajectory is bounded by these curves (tori). As clearly seen for the system at the top, a typical reactive trajectory (a trajectory capable of crossing the barrier) only visits a restricted region of configuration space; moreover, it tends to recross the barrier quite frequently and sometimes periodically. For this system, the amount of time a typical trajectory spends in a well is not long (relative to the period of oscillation across the well); therefore, "trapping" for long periods of time does not occur, and a phenomenological rate constant does not exist for this system. The corresponding reactive flux in the second column indeed confirms this notion. It is oscillatory about 0 with nonexponential long time decay. In the middle system of Fig. 1, a much wider area of configuration space is sampled by a typical trajectory. It is now possible for a trajectory to become trapped for long periods of time. Nevertheless, note that a trajectory cannot cover all of the available configuration space. The corresponding reactive flux in the second column approximately decays at long times with only one decay constant. If one now assumes that this long time decay is exponential, then a rate constant may be extracted. This decay rate turns out to be significantly smaller than the value predicted by RRKM theory. Consider the final system at the bottom of Fig. 1. A typical reactive trajectory tends to fill all of the available configuration space. Trapping times are very long (on the order of 100 vibrational periods). Not only does one obtain a reactive flux that is almost a pure exponential, but one also finds that the decay is given, within error, by the RRKM value [cf. Eq. (4)]. As expected, a necessary condition for RRKM theory to be valid is that the entire energy hypersurface must be irregular and furthermore, that it not be decomposable.

Upon close examination, one finds that the primary difference between the three systems is that the measure of the regular region of phase space (tori) decreases from the first to last system. For the last system, no integrable regions were found at an energy of 1.02. In particular, it was found that if tori still existed at the energy of interest, then one could obtain long-lived correlations within a trajectory due to remnants of the destroyed tori—or so-called vague tori.[11]

Clearly then, it would be valuable if there were some method by which one could predict when the last vestige of integrability vanished. Should this happen for an energy lower than the barrier, the system will be completely irregular above the barrier, and RRKM theory is expected to be valid. Such a method would then allow one to predict when RRKM theory is applicable. For a given system, we will be interested in determining that energy at which all regularity disappears. This energy will be labeled E_{RRKM}. Clearly,

$$E_{\mathrm{RRKM}} > E_{\mathrm{CRIT}} , \tag{5}$$

where E_{CRIT} is the energy at which nonintegrability (irregularity) first appears macroscopically. In the next section, we study a simple method by which we can obtain a lower bound on E_{RRKM}; a lower bound that is still greater than E_{CRIT}. Let this lower bound be labeled E_{SU}, then

$$E_{\mathrm{RRKM}} > E_{\mathrm{SU}} > E_{\mathrm{CRIT}} . \tag{6}$$

In the next section, we use linear stability analysis to determine E_{SU}.

In closing this section, it should be mentioned that microcanonical rate constants in general and the RRKM rate constant in particular can exist only for energies close to the barrier. This is a necessary condition, since, at higher energies, the transition state will usually be much too wide for a sufficient separation in time scales to occur, and there will then be rapid recrossings of the energy barrier (cf. Ref. 2). In other words, one must have an efficient bottleneck to reaction.

IV. LINEAR ANALYSIS

Consider the classical Hamiltonian

$$H=4(\dot{x}^2+\dot{y}^2)+4y^2(y^2-1)F(x)+4\omega_0^2x^2+1\ . \qquad (7)$$

This Hamiltonian represents a quartic bistable oscillator coupled to a harmonic oscillator via the function $F(x)$. This Hamiltonian has been expressed in dimensionless units, so that the unperturbed barrier height is 1.0. The frequency factor ω_0 is actually the ratio of the unperturbed frequency of motion in the harmonic mode to the harmonic frequency of the unperturbed bistable mode.

In general, the phase space of the system can be decomposed into irregular and regular regions (cf. Fig. 1). As the energy is increased, the measure of the regular region changes (usually decreases). The regular regions are each nested about a single trajectory that defines an elliptic fixed point. As long as a single elliptic fixed point exists, there is at least a small measure of nested tori about it. As the energy is increased, an energy is reached for each of these single elliptic points at which they become hyperbolic fixed points. For each such elliptic point, linear stability analysis can be used to determine the energy at which this transition occurs.[12] It is important to note that at these energies, the system may still be globally stable, i.e., quasiperiodic. It is reasonable to conjecture that *for the energy E_{SU}, at which the most stable elliptic point becomes linearly unstable, all the other elliptic fixed points will also be unstable.* A small increase in energy above E_{SU} will lead to global instability of this elliptic fixed point and consequently by the disappearance of all regularity. Of course, the transition of an elliptic point to a hyperbolic point *does not* guarantee that global chaos will in fact ensue. It is a simple matter to vary the parameters of a given Hamiltonian system until the above transition does not represent forthcoming chaotic behavior. What we would like to emphasize instead is that, in general, it has been *our experience* that this transition is a good indicator that the dynamical system may be in the process of becoming highly unstable—it certainly does not guarantee this, but it does give us an important gauge. It is not *a priori* clear which elliptic fixed point, for a given system, is the most stable. Here, it will be assumed that the most stable elliptic point is generated by the trajectory which oscillates in the X direction about the well with no motion of the Y coordinate. The initial conditions for this trajectory is $(x, \dot{x}, \dot{y}=\sqrt{1/2}, y=0)$. Under these initial conditions, this trajectory is always stable, but small perturbations about it may or may not be. Thus, the question of when the two-dimensional motion becomes totally stochastic is approximately reduced to the well-studied problem of the analysis and prediction of stability of one-dimensional motion.[12–14] Again it should be emphasized that this condition is only necessary, but not sufficient.

If we make the transformation from the (x, y) coordinate system to the coordinate system (q, X), where $y=1/\sqrt{2}+q$, and then linearize the resulting differential equation in q,[12] we obtain

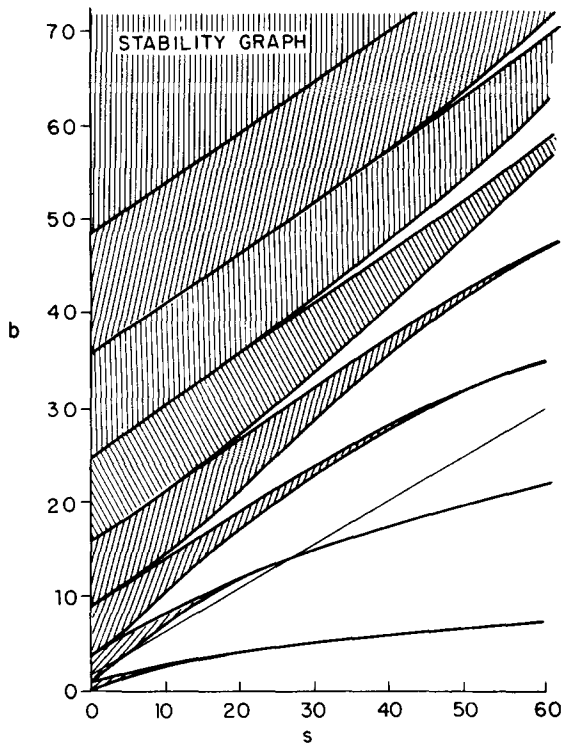

FIG. 2. This figure gives the stability graph for the Mathieu equation [cf. Eq. (9)]. The hatched regions correspond to stable regions. The line at the bottom is given by $b=1.5+0.5\,S$. It is the example cited in the text.

$$\ddot{q}=-2F[X(t)]q\ , \qquad (8a)$$

$$\ddot{X}=-\omega_0^2X+(dF(X)/dX)/8\ , \qquad (8b)$$

Note that Eq. (8b) is not coupled to Eq. (8a). If the solution to Eq. (8b) is periodic, then Eq. (8a) is the general form of Hill's equation. Therefore, our task is reasonably straightforward; we first solve Eq. 8(b), use this to determine $F(t)$ and then determine the stability of Eq. (8a). Unfortunately, in general, it is not possible to analytically determine the stability of Hill's equation.[15] Nevertheless, for certain forms of $F(x)$ we can obtain Mathieu's equation, which is a particular type of Hill's equation, from Eq. (8a). The regions of stability and instability for the Mathieu equation may be obtained from

$$\ddot{q}+[b-S\cos^2(t)]q=0\ , \qquad (9)$$

where b and S are parameters. The stability graph of Eq. (9) is usually displayed in a b versus S plane (cf. Fig. 2).[16]

In the following model problem, we obtain the Mathieu equation by letting the coupling function $F(X)$ take on the form

$$F(X)=1-ZX\ . \qquad (10)$$

This choice of $F(X)$ has similar properties to the choice of $F(X)$ in Ref. 2. That is, the effective barrier height decreases as the transverse degree of freedom X is stretched. If we insert Eq. (10) into Eq. (8), one obtains for the uncoupled solution

$$X(t)=A\cos(\omega_0t+\delta)-Z/(8\omega_0^2)\ . \qquad (11)$$

Here

$$A = \frac{1}{2\omega_0}\sqrt{E + Z^2/(16\omega_0^2)} \tag{12}$$

and δ is just a phase factor. Equation (11) allows us to put Eq. (8a) in the form of a Mathieu equation. The result leads to the following identification of the parameters b and S:

$$b = b_0 + S/2\ , \tag{13a}$$

$$b_0 = 8[1 + 1/(8\rho^2)]/\omega_0^2\ , \tag{13b}$$

$$E = Z^4\rho^6 S^2/64 - 1/(16\rho^2)\ , \tag{13c}$$

where $\rho = \omega_0/Z$. Can the linear analysis tell us anything about the global dynamical behavior of this system? In Fig. 2, we plot a typical stability line, given by Eq. (13a) on the stability graph. The hatched regions of the stability graph correspond to stable regions. In the particular example presented, the b axis intercept b_0 is 1.5 and the value of s at which the behavior goes from linear stability to linear instability S_{SU} is 2.2. Note that all systems with the same value of b_0 will also have the same value of S_{SU}. Therefore, for a given b_0, it is the value of E_{SU} which changes as the parameters Z and ω_0 are varied. Since in the Hamiltonian [Eq. (7)], the minimum in the barrier to reaction is 1.0, if one is to destroy all tori at energies close to the barrier, then it is required that $E_{SU} < 1.0$.

In Fig. 3, we plot E_{SU} as a function of Z for the above case of $b_0 = 1.5$ (solid curve). Clearly, we cannot use values of Z much less than about 6.0, otherwise, instability does not occur at energies above the barrier and the system is not expected to exhibit RRKM-like behavior. As an example, for the case of $b_0 = 1.5$, we pick the values of $Z = 16.0$ and $\omega_0 = 4.0$. The predicted value of E_{SU} is 0.21—an energy well below the barrier. In Fig. 4, we plot the Poincare surface of section

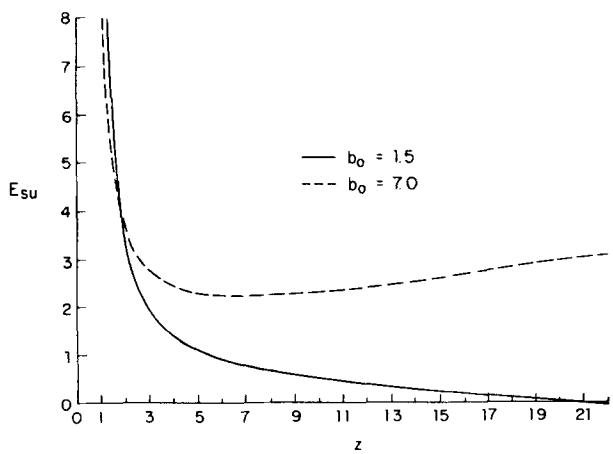

FIG. 3. The curve $E_{SU}(Z; b_0)$ vs Z is plotted for two typical values of b_0. For the solid curve $S_{SU} < 2b_0$ and hence no minimum exists. Conversely, for the dashed curve $S_{SU} > 2b_0$ and a minimum must exist [cf. Eq. (15)]. Note that systems described by the dashed curve cannot be RRKM systems; whereas, according to the solid curve, RRKM systems should exist for $Z \gtrsim 9.0$.

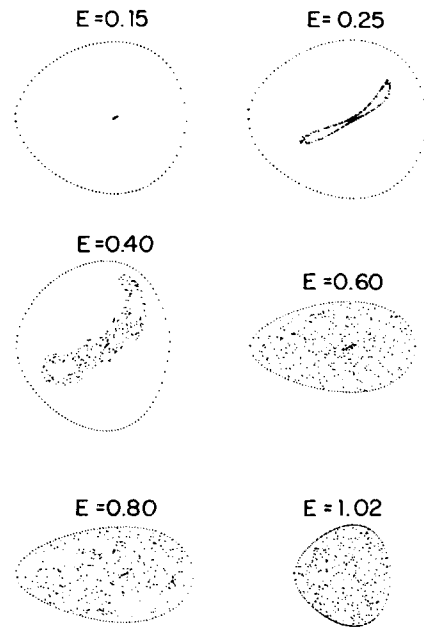

FIG. 4. Poincare surface of sections in the Y, $\dot{Y}$ plane corresponding to the linear stability analysis. The parameters for the Hamiltonian are $Z = 16.0$, $\omega_0 = 4.0$. The six sections are taken at six different energies ranging from 0.15 to 1.02. The stability analysis predicts the elliptic fixed point to become a hyperbolic fixed point at $E = 0.21$—as one indeed finds. Note that chaos is attained at an energy less than 0.6. The corresponding trajectories that generated this figure are displayed in Fig. 5.

through the plane Y, $\dot{Y}$ given $X = X$ min, $\dot{X} > 0$, (X min $= -Z(8\omega_0^2)$). $X_{\min}$ is the x component of the minimum in the potential energy surface. At an energy of 0.15, we indeed have linear stability as the elliptic fixed point at the center indicates. As the total energy is increased to 0.25, the elliptic fixed point turns into a hyperbolic fixed point, as predicted by the linear analysis. On close examination, 0.21 indeed turns out to be the transition energy. Note, however, that even though the trajectory is linearly unstable it nevertheless is globally stable. Indeed, the elliptic fixed point bifurcates into two elliptic fixed points and it itself becomes the hyperbolic point between them. This kind of bifurcation of elliptic fixed points seems to be a general phenomenon in many dynamical systems.[17] Because of this inherent stability, E_{SU} is usually a good indicator of how close we are to E_{RRKM}. For example, in Fig. 4 at an energy of 0.4, we see that the trajectory is still linearly unstable, but now somewhat globally unstable (stochasticity in the surface of section is quite noticeable). Finally, at an energy of 0.6, the trajectory is both linearly and globally unstable. Thereafter, up to and beyond an energy of 1.02, all one obtains is a shotgun-like pattern in the surface of section—one of the signatures of chaos.[18] Figure 4 indicates that if E_{SU} occurs well below the barrier, say $\lesssim 0.5$, then we can in general expect E_{RRKM} to be less than 1.0—a necessary condition for the system to have an RRKM rate constant. It is important to note that this is *not generally a sufficient condition*, due to the existence of a few small parameter ranges where it is possible that the hyperbolic point

will again become an elliptic point at energies below the barrier. We return to this possibility later.

In Fig. 5, we show the configurational trajectories used to generate the surface of sections of Fig. 4. One should compare the regularity (or lack thereof) of the trajectory and the corresponding surface of section. Note that the linear analysis allows us to predict that at an energy just above the barrier we should encounter total chaos—as the irregular trajectory at $E=1.02$ indicates. If we look back at the solid curve in Fig. 3, we can conclude that if we decrease Z below ~9.0, we should not expect to obtain complete chaos above the barrier. This indeed turns out to be the case. Therefore, we may conclude that a good conditions for global chaos to *occur above the barrier* is for E_{SU} to occur deep in the well (keeping in mind that one may find a few cases where this criterion is insufficient). We find that this latter criterion is correct for most of the parameter range considered—not just for those parameters satisfying the condition $b_0=1.5$.

The linear stability analysis allows us to construct a stability graph Fig. 6 of ω_0 versus Z for various values of b_0, that provides us with insight into which parts of parameter space correspond to RRKM-like systems. This graph was constructed by varying the value of b_0 from 0.5 to 35.0. For values of $b_0>35.0$, the system is found to be stable except in very small regions of parameter space (cf. Fig. 2). The dotted regions of Fig. 6 roughly correspond to those regions of parameter space where one will obtain an RRKM system. The criterion on E_{SU} was again chosen to be such that $E_{SU}<0.5$. There are several interesting features of this graph that should be pointed out. First, notice that for either large ω_0 ($\omega_0>4.5$) or for small ω_0 ($\omega_0<1.0$), no

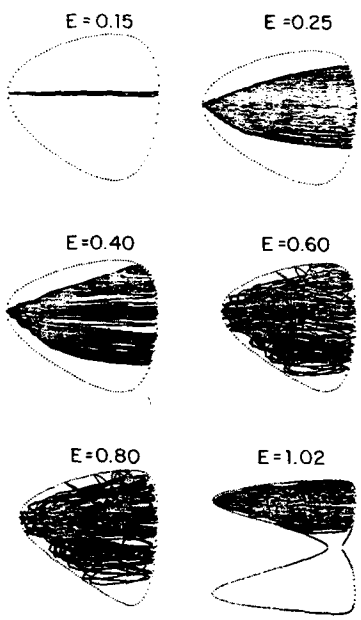

FIG. 5. These are the trajectories used to generate the surface of sections of Fig. 4. In each case, trajectories were generated with the initial condition $X=X_{min}$, $Y=1/\sqrt{2}$, $\dot{Y}=0.001$, $\dot{X}=\dot{X}(E;X,Y,\dot{Y})$. Given sufficient time, all of the trajectories at or above $E=0.6$ will fill the entire configuration space.

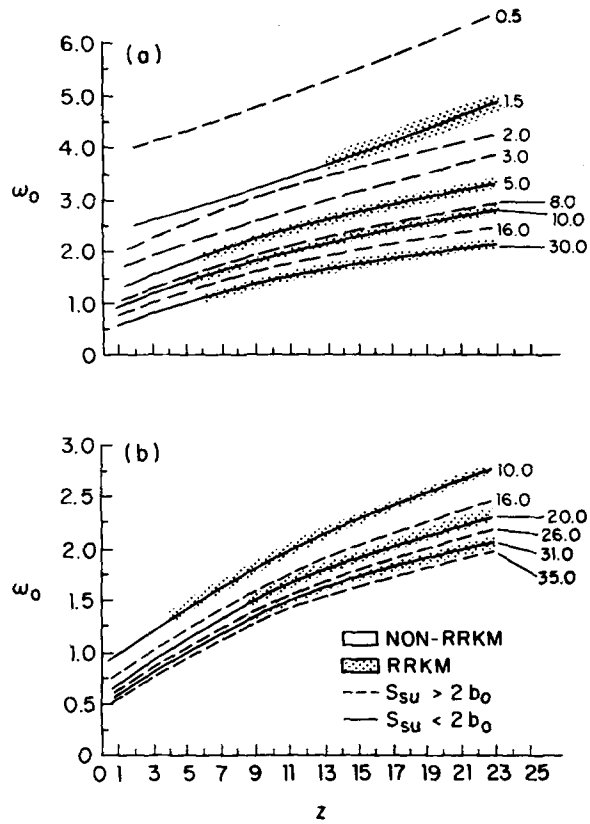

FIG. 6. This figure is the principal result of this paper. In the ω_0 vs Z plane, we plot those areas where one expects to find systems whose rate constants are accurately predicted by RRKM theory. This figure is separated into two sections. Figure 6(a) displays a wider range of the parameter space. Figure 6(b) enlarges the small ω_0 dependence of Fig. 6(a). See the text for discussion.

linear instability occurs below the barrier. We can immediately obtain the pertinent parameter space for RRKM behavior, it would be bounded by approximately

$$1.0<\omega_0<4.5\,,\qquad 3.0<Z\,. \tag{14}$$

Though the exact limits on Eq. (14) are not important, they do point out in a semiquantitative fashion that the approximate frequency in the transverse mode (x in this case) cannot be either too large or too small. In either extreme, the modes will adiabatically decouple from on another—the result being that the system again becomes integrable. This kind of behavior was observed in Ref. 2. Next, note in Fig. 6 that some of the lines of constant b_0 are solid and some are dashed. As in Fig. 3, dashed lines correspond to the function $E_{SU}(Z;b_0)$ with a minimum and solid lines correspond to the function $E_{SU}(Z;b_0)$ behaving monotonically, e.g., with no minimum. It can be shown that RRKM systems can only lie on lines of constant b_0 corresponding to the latter type. In fact, one may obtain the interesting relations,

$$S_{SU}/2>b_0,\quad \text{minimum exists},\qquad S_{SU}/2<b_0,\quad \text{minimum nonexistent}\,. \tag{15}$$

TABLE I. This table lists the values of S_{SU} for various values of b_0 extracted from Fig. 2. More precisely, the tables supplied by Ref. 16 were used to calculate S_{SU} somewhat more accurately.

b_0	S_{SU}	b_0	S_{SU}
0.05	1.75	19.00	35.24
1.50	2.20	20.00	35.40
2.00	4.90	21.00	39.60
3.00	13.75	22.00	43.90
5.00	7.25	23.00	48.20
6.00	11.70	24.00	52.90
7.00	16.90	25.00	57.90
8.00	26.00	26.00	64.00
8.80	30.60	29.00	46.90
10.00	12.60	30.00	51.80
11.00	17.40	31.00	56.00
12.00	22.00	32.00	60.00
13.00	26.40	33.00	64.20
14.00	32.20	34.00	68.40
15.00	36.70	35.00	72.70
16.00	44.40		

Table I lists various values of b_0 and the corresponding S_{SU}. Because of the above demarcation, one cannot obtain a continuous series of RRKM systems as one progresses down ω_0 for a fixed value of Z. Instead, bands of RRKM regions are obtained. The width of each band significantly decreasing as ω_0 gets smaller. One should note that the dynamical system is very sensitive to a small change in ω_0. The above point is a direct indication that nonlinear systems can in general be very sensitive to small variations in their parameters.

It should be pointed out that there are a few small ranges of ω_0 which have an E_{SU} deep in the well but with no global chaos above the barrier. This is due to a linear restabilization of the trajectory, that is, the unstable region in Fig. 2 was not "wide enough" to maintain the instability throughout the necessary energy range. For example, at $b_0 = 28.0$, there is an instability at $S_{SU} = 42.0$ and a restabilization at $S = 60.5$. This latter stability tends to maintain a semblance of global stability. Fortunately, the above case seems to be remote and in general one will not need to worry about it.

V. CONCLUSIONS

The above linear stability analysis provides us with information about the global dynamical behavior of the system. It has been demonstrated that the energy E_{SU} can be a simple quantity to calculate. The evaluation of this quantity provides us in most cases with a good estimate of E_{RRKM}, if it exists. It therefore suggests when we can expect RRKM rate constants to be accurate. In Ref. 2, it was demonstrated that the system was more sensitive to variations in ω_0 than variation in Z. The above analysis (cf. Fig. 6) is consistent with this observation, and moreover produces the same kind of dependence on ω_0. That is, for large and small ω_0, the system becomes more integrable—an observation which we have attributed to adiabatic behavior. In general, we have observed that the measure of integrable regions can be very sensitive to the parameters of the Hamiltonian—especially the frequency ratios between the two modes.

The above analysis is not restricted to the system presented in this paper. Instead, it is applicable in general. The difficulty lies, of course, in the evaluation of the stabilty of the general Hill's equation. Only for a very few cases is the stability of Eq. (8a) well studied. Nevertheless, if one wanted to carry out the linear analysis, it could be accomplished numerically by determining the linear mapping matrix $\mathbf{T}$,

$$\mathbf{Y}(\tau_n) = \mathbf{T}^{(n)}\mathbf{Y}(0)\,, \qquad (16)$$

$$\mathbf{Y}(\tau) = [\dot{y}(\tau),\ y(\tau)]\,,$$

and then determine the eigenvalues of T. The imaginary eigenvalues correspond to an elliptic point and real eigenvalues correspond to a hyperbolic point.

It is at this point proper to emphasize that the aforementioned stability analysis is only the simplest of the various techniques used to estimate when one can expect to encounter chaos in dynamical systems. Much more sophisticated techniques have been developed by Mo,[19] Cerjan and Reinhardt,[20] Kosloff and Rice,[21] Zaslavskii and Chirikov,[22] Bummer, Duff, and Toda,[23] and J. Ford.[24] In some cases, these are simple to apply but in general they tend to be very cumbersome indeed. The principal difference between the above methods and the use of the stability analysis in this paper is *that we are not trying to determine that energy for which one first observes the onset of chaos* E_{CRIT}—the principal goal of the above authors—rather, *we are interested in a less complicated energy* E_{SU} *which (we claim) can give a good indication of when the* RRKM *theory of the rate constant is accurate.* This gives a qualitative test for the validity of RRKM theory.

Another difficulty lies in determining the range of energy in which the bifurcated elliptic points remain stable. It would be very desirable if one could find a method by which their range of stability could be determined. If this were possible we would then, essentially, be able to calculate E_{RRKM} rather than E_{SU}. Needless to say, we are unaware of any method that specifically treats this though there are investigations dealing with specific systems.[17,25] Of course, one expects the bifurcated elliptic point to bifurcate again, and so on. These secondary and tertiary bifurcations need not concern us, since the energy range in which they are stable quickly decreases as the hierarchy progresses. In Fig. 6, we have approximated the energy at which the primary bifurcated elliptic points are stable to be ~ 0.5 in all cases. This is, of course, an approximation but one that is born out by direct trajectory calculations.

In spite of the above inherent difficulties in the calculation, the simple system we studied has provided us with much useful information. We believe that by avoiding the direct determination of E_{RRKM}, and, instead, focusing on E_{SU} we can provide simple but, nevertheless, instructive criterion for statistical rate theory.

ACKNOWLEDGMENT

One of us (N.D.L.) would like to thank Ms. Jennifer Costley for several helpful discussions.

[1]J. B. Montgomery, Jr., D. Chandler, and B. J. Berne, J. Chem. Phys. 70, 4056 (1979).
[2]N. De Leon and B. J. Berne, J. Chem. Phys. 75, 3495 (1981).
[3]R. O. Rosenberg, B. J. Berne, and D. Chandler, Chem. Phys. Lett. 75, 162 (1980).
[4]D. Chandler, J. Chem. Phys. 68, 2959 (1978).
[5]S. H. Northrup and J. T. Hynes, J. Chem. Phys. 73, 2715 (1980).
[6]E. Helfand, J. Chem. Phys. 69, 1010 (1978).
[7]W. Forst, *Theory of Unimolecular Reactions* (Academic, New York, 1973).
[8]W. H. Hase, *Dynamics of Molecular Collisions, Part B*, edited by W. H. Miller (Plenum, New York, 1976).
[9]M. Henon and C. Heiles, Astron. J. 69, 73 (1964).
[10]G. Benettin and J. M. Strelcyn, Phys. Rev. A 17, 773 (1978).
[11]W. Reinhardt, J. Phys. Chem. (in press).
[12]E. Thiele and D. J. Wilson, J. Chem. Phys. 33, 1256 (1961).
[13]M. J. Davis, E. B. Stechel, and E. J. Heller, J. Chem. Phys. 73, 4720 (1980).
[14]M. A. Lieberman, *Non Linear Dynamics* (Annals of the New York Academy of Sciences, New York, 1979), Vol. 357.
[14]W. Magnus and S. Winkler, *Hill's Equation* (Dover, New York, 1966).
[16]M. Abramowitz and A. Stegen, *Handbook of Mathematical Functions* (Dover, New York, 1965).
[17]M. J. Feigenbaum, Siam J. (in press).
[18]J. Ford, Adv. Chem. Phys. 24, 155 (1972).
[19]K. C. Mo, Physica (Utrecht) 57, 445 (1972).
[20]C. Cerjan and W. D. Reinhardt, J. Chem. Phys. 71, 1818 (1979).
[21]R. Kosloff and S. A. Rice, J. Chem. Phys. 74, 1340 (1981).
[22]G. M. Zaslariskii and B. V. Chirikov, Sov. Phys. Usp. 14, 549 (1972).
[23]M. Toda, Phys. Lett. A 48, 335 (1974); P. Brumer and J. W. Duff, J. Chem. Phys. 65, 3566 (1976).
[24]G. H. Walker and J. Ford, Phys. Rev. A 188, 416 (1969).
[25]T. C. Bountis, Physica D 3, 577 (1981).